

Hardware-Software Platform Enabling Joint Communication and Radar Sensing at 25 GHz with 1 GHz Bandwidth

Sandra George¹, Padmanava Sen¹, Mehrab Ramzan¹, Muhammad Umar¹, Yash Richhariya¹,
Jan Adler¹, Corrado Carta^{2,3}

¹Barkhausen Institut, Germany

²IHP Microelectronics GmbH, Germany

³Technische Universität Berlin, Germany

{sandra.george, padmanava.sen, mehrab.ramzan, muhammad.umar, yash.richhariya,
jan.adler}@barkhauseninstitut.org, carta@ihp-microelectronics.com

Abstract—Joint Communication and Radar Sensing (JCAS) is predicted to be one of the compelling features of future 6G systems. This paper presents a hardware-software evaluation platform designed to analyze JCAS performance in scenarios where multi-purpose receiver (RX) front-end, antennas, and waveforms are utilized to support both communication and sensing functionalities. The measurements are conducted in the 5G NR n258 band with 1 GHz bandwidth. The front-end is tunable in gain, linearity, and frequency and is supported by a wideband high-isolation co-located aperture coupled antenna. The RX front-end has a peak gain of 29.9 dB and achieves a maximum iP_{1dB} of -17.5 dBm for a gain of 16.8 dB. The antennas provide an isolation of more than 40 dB across the operating band. The software platform supports several types of waveforms and modulation standards enabling a comprehensive performance evaluation. The paper also presents the radar measurements in a multi-target scenario along with communication measurements.

Keywords—Joint Communication and Sensing (JCAS), receiver, high isolation antennas, hardware-software platform.

I. INTRODUCTION

Joint Communication and Sensing (JCAS) has garnered significant interest in recent years and is currently a focus of extensive research activities. It is expected to become a key feature of the future 6G ecosystem [1][2]. JCAS will offer hardware and spectrum sharing which will bring advantages in terms of size, cost, power consumption and safety of the overall system. Hardware reuse option for a JCAS implementation offers attractive solutions to integrate additional novel functionalities without necessitating new blocks. However, it comes with the challenges of different front-end requirements, operational bandwidth and self-interference management [3][4]. The possible path to solve these challenges are below:

- Introduction of a front-end and an antenna capable of supporting wider absolute bandwidth for the radar applications. Conventionally the radar will require the wider bandwidth between the two applications in order to support the range resolution requirements of applications.
- A reconfigurable front-end architecture that can switch between high linearity to high gain modes in the receiver. The high linearity mode is needed to support

the close target detection in radar. In both modes, the receiver linearity should be able to handle the self-interference coming from the transmitter.

- Antennas equipped with isolation across the band that will avoid saturation of the receiver and an overall self-interference cancellation methodology to support the mono-static radar operation and as needed for In-Band Full-Duplex (IBFD) JCAS architecture.

Experimental evaluations until now were carried out with a combination of standard and custom hardware [4][5][6][7][8][9]. In [4], a custom hardware design with separate antennas for Transmitter (TX) and Receiver (RX) with a bandwidth of 245.76 MHz was presented. In [10] a platform for radar supporting up to 1 GHz bandwidth was introduced. This paper enhances the state-of-the-art evaluation platforms with the following contributions while addressing aforementioned three enablers:

- Using a receiver on Printed Circuit Board (PCB) with the chip implemented in 22FDX Global Foundries process and TX-RX antenna that can support 1 GHz of absolute bandwidth at 25.5 GHz center frequency in the 5G NR band.
- The receiver capable of switching between high gain/low linearity (Mode1) and low gain/high linearity (Mode2).
- A self-interference cancellation methodology embedded in the link level system evaluator, in addition to the 40 dB isolation from the antenna across the band.

The platform presented in the work is tested considering a mono-static radar and time-division-duplex (TDD) communications using the same hardware. However, it will also work for IBFD JCAS including IBFD communication and IBFD radar (active and mono-static).

Section II of this paper describes the different building blocks of the system. Section III provides the measurement results and section IV concludes the paper.

II. SYSTEM DESCRIPTION

The hardware-software evaluation platform in radar mode is depicted in Fig. 1 with a custom RX front-end and wideband co-located high-isolation aperture coupled antennas (ACA).

working frequency regime. The measured realized gain is approximately 7 dBi, attributed to the losses due to the connectors, substrate and fabrication tolerance at 25.85 GHz.

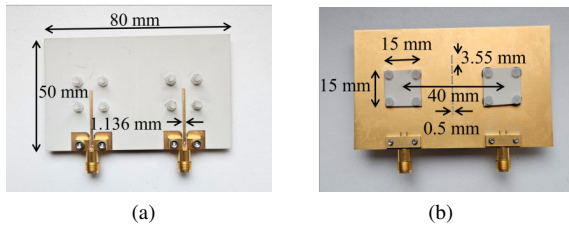


Fig. 5. Fabricated design with highlighted dimensions of co-located ACA: (a) bottom; (b) top.

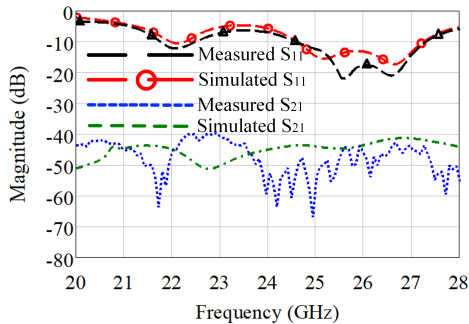


Fig. 6. Simulated and measured reflection and transmission coefficients of the co-located ACA.

C. Software Evaluation Platform

For integrating the hardware and software platforms, a USRP X440 was used. This device facilitates high-performance, multichannel wideband signal generation and analysis. HermesPy is utilized to generate and process the transmission and reception waveforms at 1 GHz intermediate frequency and 1 GHz sampling rate with an oversampling of 4 and an LO frequency of 25.3 GHz. The generated evaluation waveform is a root-raised cosine (RRC) single carrier waveform with an effective bandwidth of 900 MHz. The waveform's modulation order and frame structure, i.e. number of pilot and data symbols, are freely configurable. In order to estimate a range-power profile, HermesPy is configured to correlate transmitted frames with their respective digital counterparts sampled at receiving antennas, resulting in a range resolution of approximately 16 cm.

III. MEASUREMENT RESULTS

A. LNA measurement results

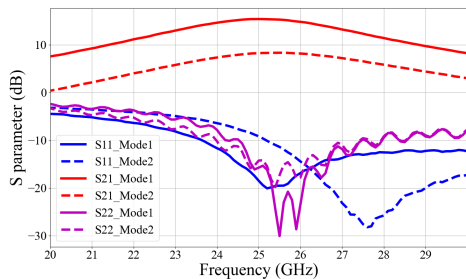


Fig. 7. Measured S-parameters of the tunable LNA in Mode1 and Mode2 for same varactor voltages.

The LNA achieves a maximum gain of 15.4 dB while consuming 13.6 mW of DC power from a supply voltage of 0.8 V during on-wafer measurements. The measured input compression point (iP_{1dB}) is at -14.1 dBm. The S-parameter measurement results for the two modes of operation are shown in Fig. 7. The measured noise figure (NF) in Mode1 is 3.1 dB at 25 GHz. To support Mode2, the bias voltage of the transistors are reduced and the LNA attains a gain of 8.3 dB and an iP_{1dB} is -5.2 dBm while consuming a total power of 2.9 mW. The NF at 25 GHz in this mode is 3.8 dB.

B. Receiver PCB characteristics

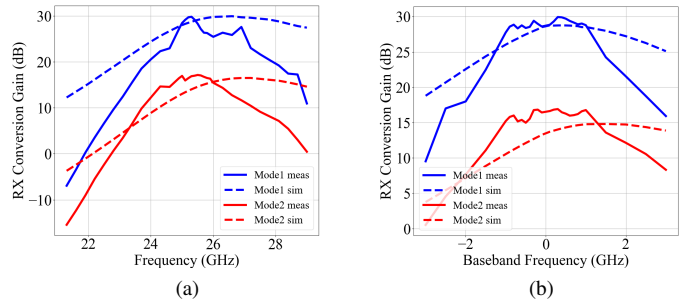


Fig. 8. Receiver characteristics (a) RX conversion gain Vs RF frequency at BB 300 MHz; (b) RX conversion gain Vs BB frequency at a constant LO of 25 GHz.

The peak conversion gain of the receiver in Mode1 is 29.93 dB, while the iP_{1dB} is at -34 dBm. The peak conversion gain in Mode2 is 16.8 dB at 25.3 GHz with an iP_{1dB} of -17.5 dBm. The measured and simulated RX characteristics with respect to RF frequency with a fixed baseband frequency of 300 MHz is shown in Fig. 8a. The conversion gain characteristics with respect to the baseband at a fixed LO of 25 GHz is shown in Fig. 8b and the receiver achieves a bandwidth of 2.5 GHz in baseband. An LO power of 2.5 dBm was used for all measurements.

C. Radar Measurements

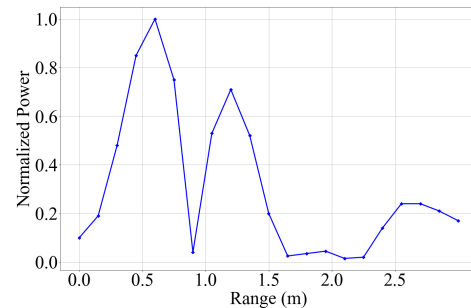


Fig. 9. Radar range measurements in a multi-target with targets separated by a distance of 0.60 m.

In order to test the sensing capabilities of the proposed hardware-software platform, two corner reflectors were placed at a respective distance of 60 cm and 120 cm from the transceiver. The resulting normalized range power profile is visualized in Fig. 9. Due to the two distinct peaks, both targets are clearly distinguishable.

D. Communication Measurements

The performance of the platform was evaluated in communication mode with co-located ACA on both RX and TX sides. Measurements were also done with a highly directive horn antenna with a gain of 13 dBi to study the antenna effects. The TX and RX antennas were placed in a LOS arrangement with 0.5 m separation. The symbol rate for the waveform was 250 MSymbols/s. The eye and constellation diagrams for the custom receiver and antennas are shown in Fig. 10 for a Quadrature Phase Shift Keying (QPSK) modulated signal with a bit rate of 500 Mbps. The RX chain performances as constellation diagrams with ACA and horn antennas for an 8 Phase Shift Keying (8-PSK) modulated signal with a bit rate of 750 Mbps are shown in Fig. 11. The narrowband and wideband Signal-to-Noise Ratio (SNR) showed a degradation of 5.8 dB for ACA as compared to the narrowband and wideband SNR of 33.65 dB and 30.9 dB of the horn antennas respectively. This can also be observed in the tighter constellation points in Fig. 11b. The Bit Error Rate (BER) for all scenarios was zero. Despite the comparatively high SNR, the broad constellation points can be explained by the lack of equalization at the receiver.

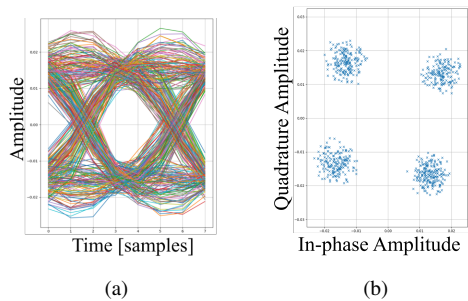


Fig. 10. Communication mode measurements at modulation order 4 with co-located ACA: (a) Eye diagram; (b) Constellation.

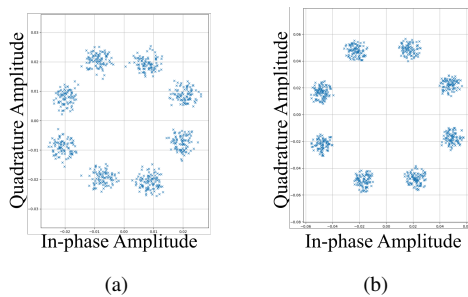


Fig. 11. Communication mode constellation diagram measurements at modulation order 8 with: (a) co-located ACA; (b) Horn antennas.

IV. CONCLUSION

This paper presents a tunable receiver along with a TX-RX antenna which can support a bandwidth of 1 GHz for JCAS applications. The antenna achieves over 40 dB isolation within the band, which is crucial for self-interference cancellation and helps prevent receiver saturation. The hardware was validated and compared using the software evaluation platform under different modulation orders. The paper thus provides an improved solution for JCAS implementations and addresses requirements of the RF front-end, bandwidth and self-interference management.

ACKNOWLEDGMENT

This work is funded by the German Federal Ministry of Education and Research under the KOMSENS-6G project with the grant number 16KISK122. The responsibility for the content of this publication lies with the author. It is also financed with tax revenue on the basis of the budget approved by the Saxon state parliament.

REFERENCES

- [1] C. De Lima, D. Belot, R. Berkvens, A. Bourdoux, D. Dardari, M. Guillaud, M. Isomursu, E.-S. Lohan, Y. Miao, A. N. Barreto, M. R. K. Aziz, J. Saloranta, T. Sanguanpuak, H. Srieddeen, G. Seco-Granados, J. Suutala, T. Svensson, M. Valkama, B. Van Liempd, and H. Wymeersch, "Convergent Communication, Sensing and Localization in 6G Systems: An Overview of Technologies, Opportunities and Challenges," *IEEE Access*, vol. 9, pp. 26902–26925, 2021.
- [2] M. Nemati, Y. H. Kim, and J. Choi, "Toward Joint Radar, Communication, Computation, Localization, and Sensing in IoT," *IEEE Access*, vol. 10, pp. 11 772–11 788, 2022.
- [3] S. George, P. Sen, and C. Carta, "Realizing Joint Communication and Sensing RF Receiver Front-Ends: A Survey," *IEEE Access*, vol. 12, pp. 9440–9457, 2024.
- [4] S. George, P. Sen, M. Umar, M. Matthé, J. Adler, M. Ramzan, and C. Carta, "Over-the-air 26GHz Receiver Hardware-Software Evaluation towards Joint Communication and Radar Sensing," in *2024 54th European Microwave Conference (EuMC)*, 2024, pp. 509–512.
- [5] P. Kumari, S. A. Vorobyov, and R. W. Heath, "Adaptive virtual waveform design for millimeter-wave joint communication–radar," *IEEE Transactions on Signal Processing*, vol. 68, pp. 715–730, 2020.
- [6] S. D. Liyanaarachchi, C. B. Barneto, T. Riihonen, and M. Valkama, "Experimenting Joint Vehicular Communications and Sensing with Optimized 5G NR Waveform," in *2021 IEEE 93rd Vehicular Technology Conference (VTC2021-Spring)*, 2021, pp. 1–5.
- [7] Q. Zhang, Z. Feng, and P. Zhang, "Hardware Testbed Design and Performance Evaluation for ISAC Enabled CAVs," in *Integrated Sensing and Communications*. Springer, 2023, pp. 567–586.
- [8] N. Souzandeh, M. Harifi-Mood, J. Pourahmadazar, S. Aïssa, and S. O. Tatu, "mm-wave joint sensing and communication system," in *2023 20th European Radar Conference (EuRAD)*, 2023, pp. 274–277.
- [9] Q. Zhang, K. Ji, Z. Wei, Z. Feng, and P. Zhang, "Joint Communication and Sensing System Performance Evaluation and Testbed: A Communication-Centric Approach," *IEEE Network*, vol. 38, no. 5, pp. 286–294, 2024.
- [10] C. Karle, M. Neu, B. Nuss, J. Chen, L. Witte, A. Scheder, T. Harbaum, and J. Becker, "Modular hardware design for high-performance mimo-capable sdr systems to accelerate 6g development," in *2024 IEEE 37th International System-on-Chip Conference (SOCC)*, 2024, pp. 1–6.
- [11] J. Adler, T. Kronauer, and A. N. Barreto, "Hermespy: An open-source link-level evaluator for 6g," *IEEE Access*, vol. 10, pp. 120 256–120 273, 2022.